Electronic Supplementary Material (ESI) for ChemComm.


Supporting information

# Energy level regulation of anion via hydrogen bonds effect to construct stable solid electrolyte interface for high-stability lithium metal anode

*Chuan Wang, Sheng Liu , Xinxiang Wang, Guilei Tian, Fengxia Fan, Pengfei Liu, Shuhan Wang, Chenrui Zeng, and Chaozhu Shu**

College of Materials and Chemistry & Chemical Engineering, Chengdu University of Technology, 1# Dongsanlu, Erxianqiao, Chengdu 610059, Sichuan, P. R. China1, Email address: czshu@imr.ac.cn (C. Shu).

## Experimental section

### 1. Materials

Lithium bis((trifluoromethyl)sulfonyl)azanide (LiTFSI) was purchased from Shanghai Macklin Biochemical Co., Ltd. Lithium iron phosphate($LiFePO_4$) was purchased from Suzhou Duoduo Chem Technology Co., Ltd, without coating carbon. N-methylpyrrolidone (NMP), polyvinylidene fluoride (PVDF) were purchased from Sigma-Aldrich. $LiFePO_4$ powder, PVDF and acetylene black were mixed with a mass ratio of 8:1:1 and dispersed into NMP to form a uniform slurry, then the slurry was coated on aluminum foil and dried at 120 °C for 8 h to obtain $LiFePO_4$ cathode. The mass loading of $LiFePO_4$ is about 6 mg $cm^{-2}$.

### 2. Electrochemical experiments

Electrochemical experiments were performed on the battery testing system (LAND-CT2001A). The CE was tested in Li||Cu cells, deposited of 0.5 mAh $cm^{-2}$ Li on Cu foil at 0.5 mA $cm^{-2}$ and 1 mA $cm^{-2}$ respectively, then stripped to 1 V at 0.5 mA $cm^{-2}$ and 1 mA $cm^{-2}$ respectively. Rate performance of full cells was evaluated from 1 to 5 C in various electrolytes within 2.5-4.0 V. Cycling performance of full cells was evaluated at 1 C. All electrochemical tests were taken on multi-channel electrochemical workstation (Bio-Logic VMP3). Cyclic voltammetry (CV) was performed with Li||Cu cells (potential range: -0.15-0.4 V; scan rate: 0.5 mV $s^{-1}$). Electrochemical impedance spectroscopy (EIS) tests were performed with Li||Li cells (frequency range: 10 mHz ~ 100kHz; voltage amplitude: 10 mV). Ionic conductivity of electrolytes was measured using symmetric stainless steel||stainless steel cells by collecting the electrochemical

impedance (R) at room temperature, and the conductivity was calculated using the formula that: $\sigma = \frac{L}{R \times S}$, where σ is ionic conductivity, S is the effective area of electrode, L stands for the distance between two stainless-steel electrodes.

**3. Characterizations**

The $^{7}$Li nuclear magnetic resonance (NMR) spectra were recorded on a Bruker 600MHz spectrometer. The deuterated chloroform ($CDCl_3$) was employed as the dispersion to lock field of electrolyte and the total mass of the electrolyte in NMR experiments is *ca.* 80 mg. In-deep X-ray photoelectron spectroscopy (XPS) measurement was performed on scanning X-ray microprobe (Thermo Fischer, ESCALAB 250Xi). Scanning electron microscopy (SEM, Zeiss Gemini 300) was used to monitor the morphology evolution of Li. Atomic force microscopy (AFM, Bruker Dimension ICON) and confocal laser scanning microscopy (CLSM, KEYENCE VK-X150) were used to monitor the microstructure of Li deposition layer.

**4. DFT calculations**

The geometry of studied molecule was optimized via Gaussian 1 with ultrafine integration grids at Lee–Yang–Parr gradient-corrected correlation functional (B3LYP) hybrid functional with Grimme's DFT-D3(BJ) empirical dispersion correction4 . The basis set 6-311G** basis set was selected for structural optimization.

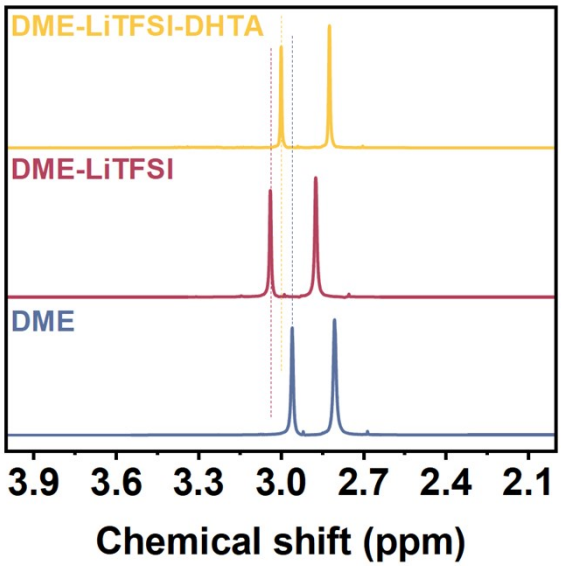


**Figure S1.** The $^{1}H$ NMR spectra of DME in $CHCl_3$ without or with presence of DHTA and LiTFSI.

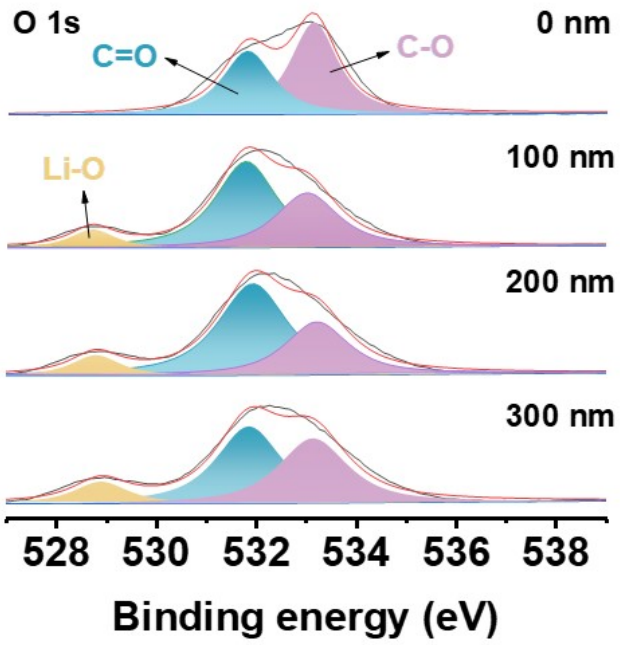


**Figure S2.** O 1s XPS depth profiles of SEI formed in DLF electrolyte.

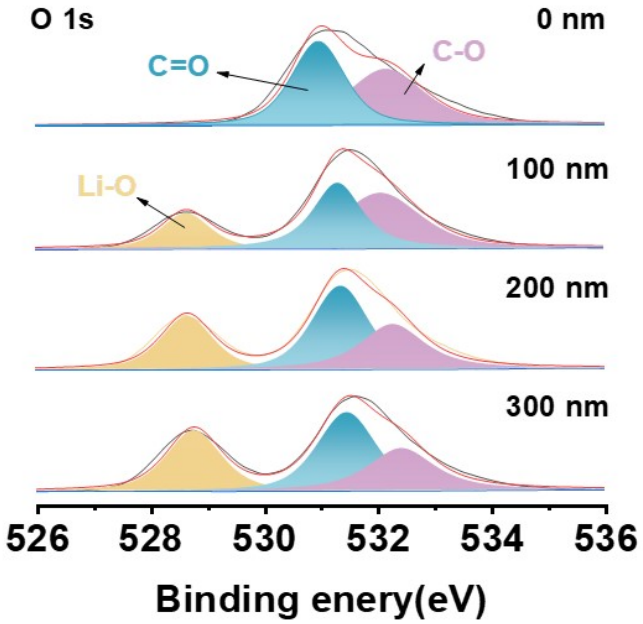


**Figure S3.** O 1s XPS depth profiles of SEI formed in DDH electrolyte.

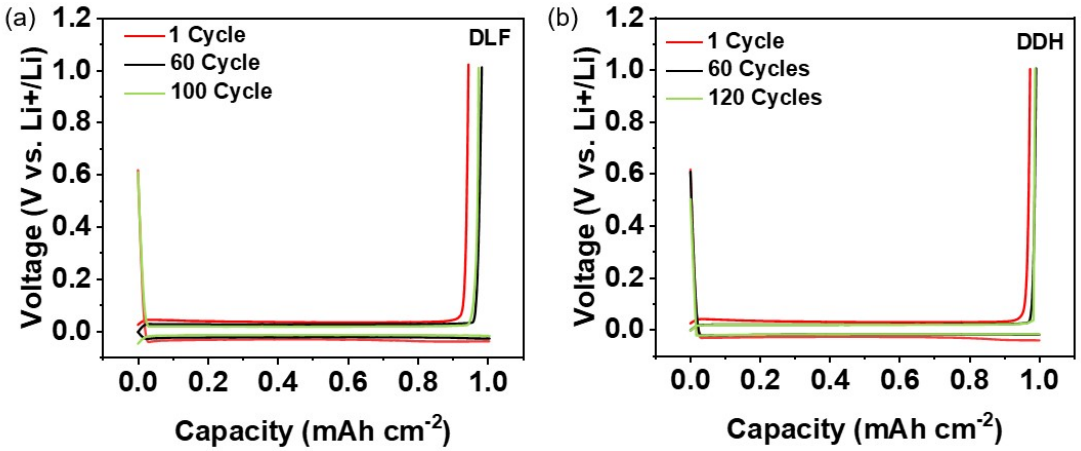


**Figure S4.** Capacity-voltage curves of the cell with (a) DLF and (b) DDH electrolytes at selected cycles.

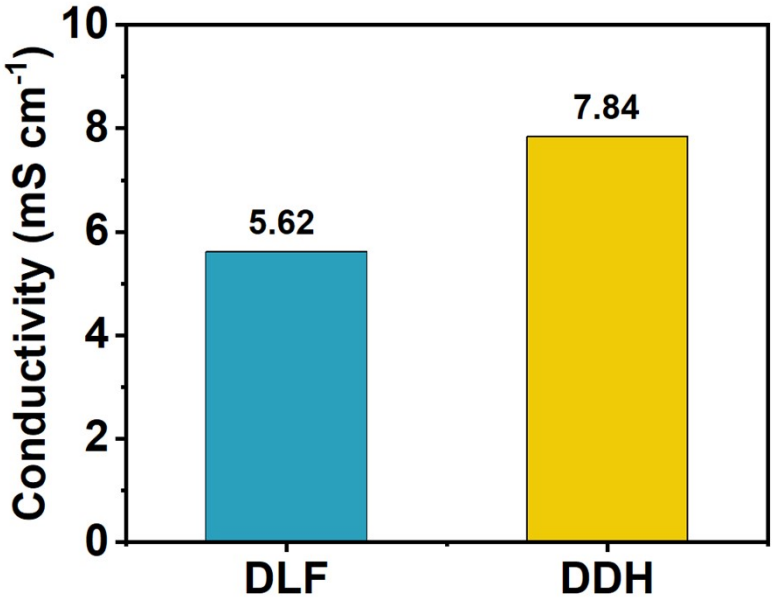


**Figure S5**. Comparison of the $Li^+$ ion conductivity of DLF and DDH electrolytes.

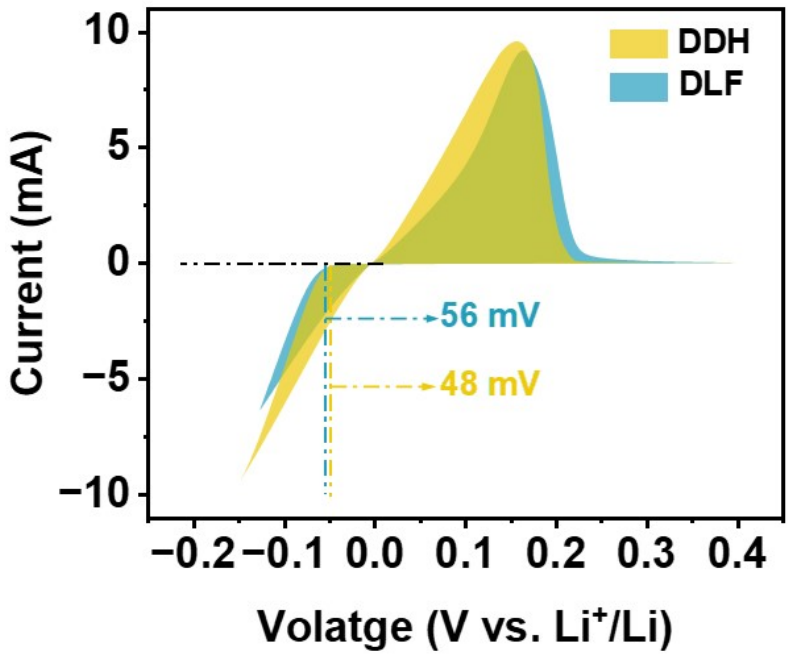


**Figure S6.** CV profiles of Li||Cu cells with DLF and DDH electrolytes.

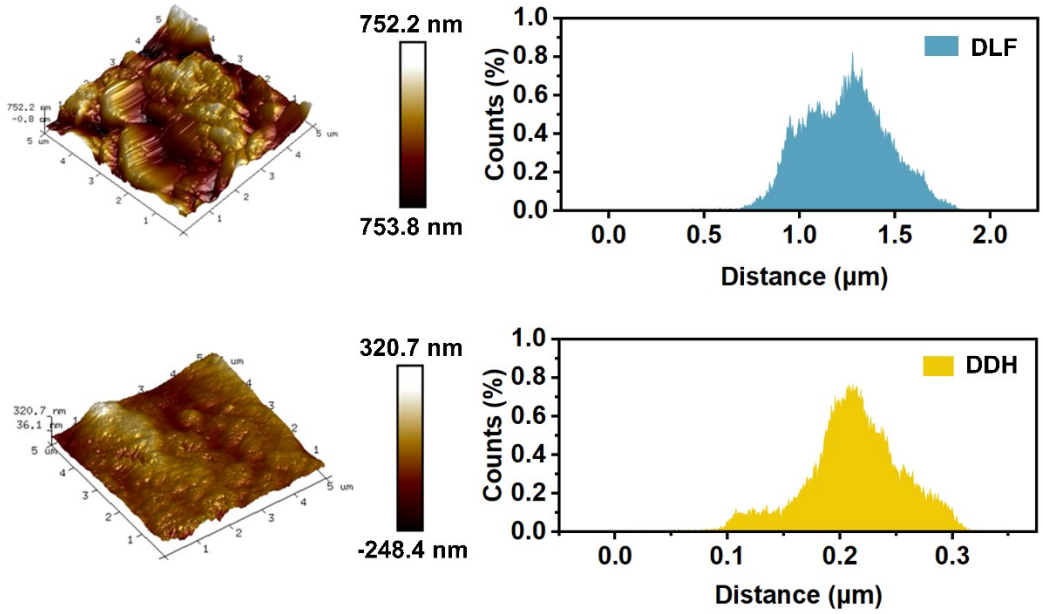


**Figure S7.** AFM images and quantitative analysis of roughness for 5 mAh $cm^{-2}$ Li deposition on Cu electrode in DLF and DDH electrolytes.

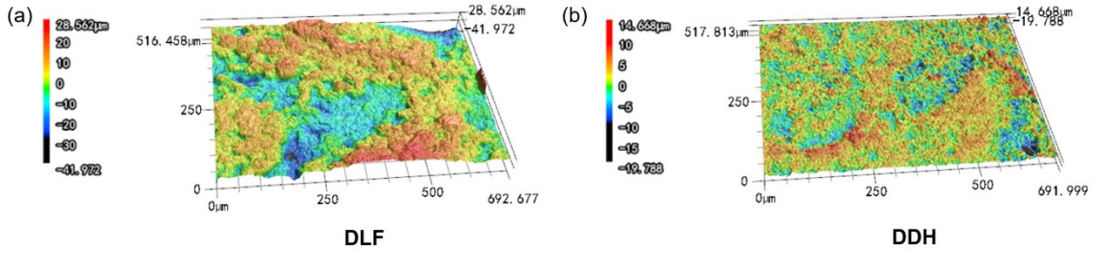


**Figure S8.** Confocal laser scanning microscopy images for 5 mAh $cm^{-2}$ Li deposition on Cu electrode in (a) DLF and (b) DDH electrolytes.

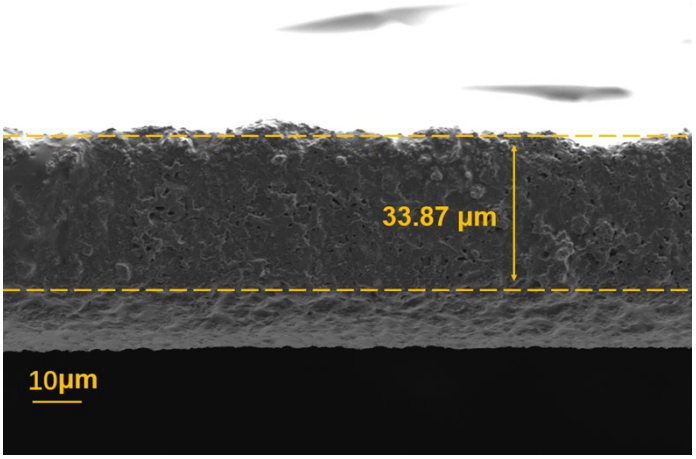


**Figure S9.** the cross-sectional SEM images of Li@Cu anode.

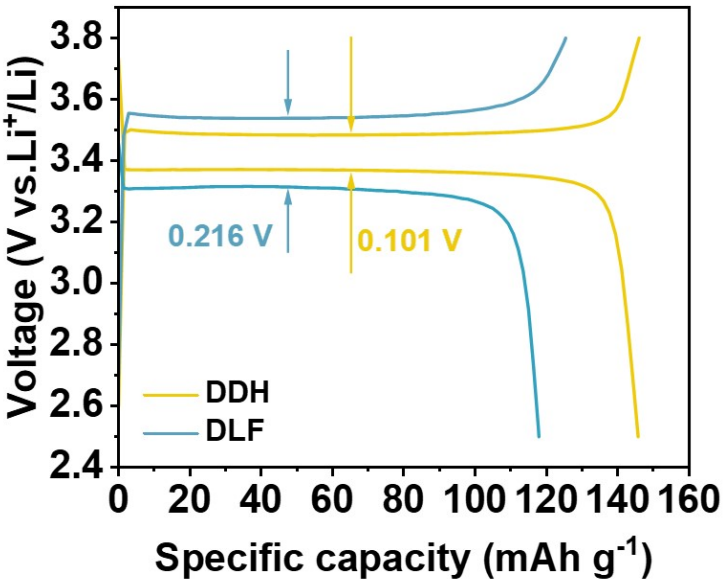


**Figure S10.** Charge/discharge curves of Li||LFP full cells in DDH and DLF electrolytes.

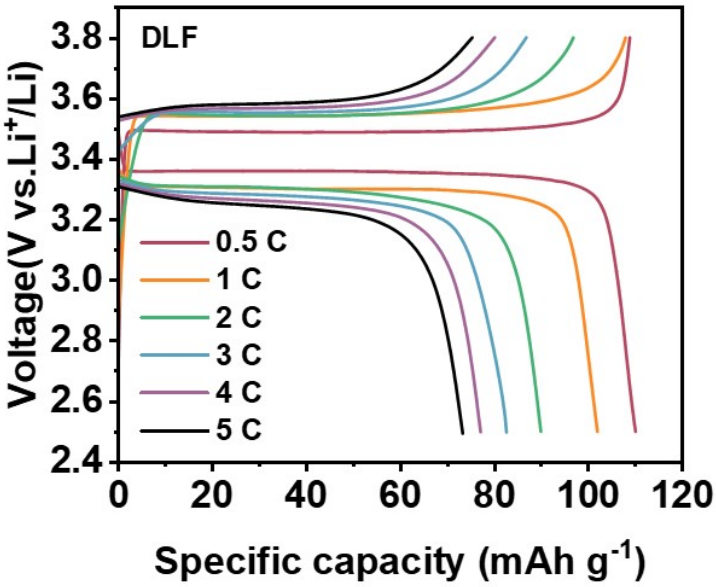


**Figure S11.** Voltage-capacity profiles of Li||LFP full cells in DLF electrolytes at different rates.

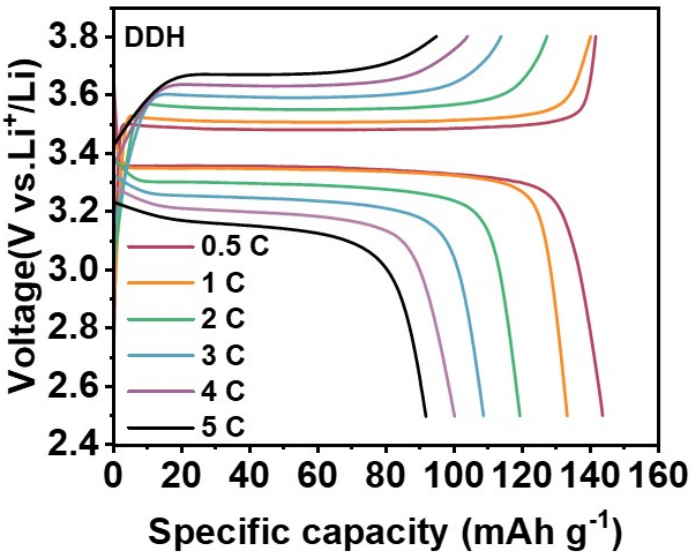


**Figure S12.** Voltage-capacity profiles of Li||LFP full cells in DDH electrolytes at different rates.